



Naphthalene diimide carrying two cysteine termini at both imide linkers as a molecular staple

著者	Sato Shinobu, Yamamura Kosuke, Takenaka Shigeori
journal or publication title	Electroanalysis
volume	25
number	8
page range	1831-1839
year	2013-07-03
URL	http://hdl.handle.net/10228/5810

doi: [info:doi/10.1002/elan.201300209](https://doi.org/10.1002/elan.201300209)

Naphthalene diimide carrying two cysteine termini at both imide linkers as a molecular staple

Shinobu Sato, Kosuke Yamamura, Shigeori Takenaka*

Department of Applied Chemistry, Kyushu Institute of Technology, Kitakyushu, Fukuoka 804-8550, Japan

* e-mail: shige@che.kyutech.ac.jp

Received: ((will be filled in by the editorial staff))

Accepted: ((will be filled in by the editorial staff))

Abstract

Naphthalene diimide **1** carrying cysteines at the termini of amide substituents were synthesized to act as a molecular staple of double strand DNA. Since **1** is able to bind to double strand DNA with threading intercalation, the complex of **1** with double strand DNA can be topologically immobilized on a gold surface through the S-Au linkage as confirmed by cyclic voltammetric experiment. Ferrocenyl-double stranded 23-meric oligonucleotide, dsFcODN, was immobilized on gold electrode with 1.0×10^{12} molecules cm^{-2} when electrode was treated with $2.0 \mu\text{M}$ dsFcODN and $4.0 \mu\text{M}$ **1** for 1 h at room temperature. The coverage density was similar to that obtained for the terminal thiol-modified oligonucleotide. Compound **1** was applied to detect the 321-meric PCR product of *P. gingivalis*, which is important in the diagnosis of periodontal disease. This experiment, coupled with the use of ferrocenylnaphthalene diimide, FND as electrochemical indicator for double stranded DNA, resulted in quantitative detection of PCR product within the range of $10 \text{ pg } \mu\text{L}^{-1} - 10 \text{ ng } \mu\text{L}^{-1}$ ($15 \text{ nM} - 15 \mu\text{M}$). The **1** and FND established a simple and rapid detection method of double strand PCR product with a detection limit of $10 \text{ pg } \mu\text{L}^{-1}$ (15 nM).

Keywords: DNA immobilized electrode, Naphthalene diimide, cysteine, molecular staple

DOI: 10.1002/elan.((will be filled in by the editorial staff))

1. Introduction

Polymerase chain reaction (PCR) is one of the most powerful tools to detect minute amounts of DNA such as influenza and SARS to prevent virus pandemics. PCR technology always requires gel electrophoresis [1] or fluorescence instrument such as in real time PCR [2]. Gel electrophoresis is an established technology, however, it is a procedure that demands a lot of time and additional steps in the protocol thus it is at some point inconvenient for most researches. On the other hand, real time PCR has been viewed as more convenient and reliable tool than the end-point traditional PCR since it monitors in “real time” the PCR product through fluorescence dye technology. Theoretically, PCR can specifically amplify target DNA and therefore detection of target DNA can be achieved [3]. However, instrumentation and fluorescence reagents are still expensive. Additionally, fluorescence dyes are easily decomposed by light. If one can develop a simple, inexpensive and rapid method to detect double strand DNA, then detection of PCR product will be much faster and at a low cost. According to these advantages,

electrochemical gene detection method has been developing by many researchers as described by the excellent reviews [4, 5]. On the other hand, recently, as DNA immobilization technique on the gold surface, acridine [6] or ethidium bromide [7] carrying thiolated alkyl chain were utilized as DNA adsorbing SAMs. However, they were based on intercalation, which is reversible and DNA cannot be fixed on their surface strongly enough.

We have developed naphthalene diimide, **3**, (Figure 1A) having two dithiolane moieties at its substituted termini as double strand DNA immobilizing reagent on the gold surface [8]. This ligand **3** bound to double strand DNA with threading intercalation and dithiolane is known to adsorb on the gold surface through chemical adsorption. We found out this ligand bound to double strand DNA and the resulting complex immobilized on the gold surface through the terminal dithiolane moieties. This can be like a molecular staple. Using this technique, DNA probe carrying 20-meric single strand DNA having complementary DNA sequence and the double strand DNA were immobilized on the gold electrode using the

ligand **3** and electrochemical DNA detection was carried out on this electrode coupled with ferrocenylnaphthalene diimide (FND) as an electrochemical indicator of double strand DNA [9-13].

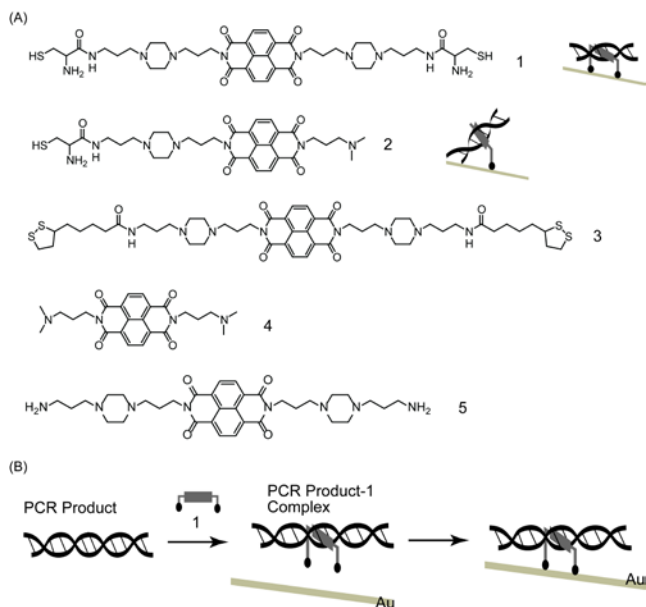


Figure 1. (A) Chemical structure of **1** and **2** and the expected immobilization of their complex with double stranded DNA (dsDNA) and (B) strategy of specific immobilization of PCR product by **1** as a DNA staple.

In this paper, we developed naphthalene diimide derivative carrying cysteine moieties at its termini, **1**, (Figure 1A) to achieve improved affinity for double strand DNA and to obtain a more effective immobilization of double strand DNA on the gold electrode. Alkane thiol is known to exhibit 50-times higher SAM formation rate than that for disulfide [14]. Although **3** have no high water-solubility, new **1** is expected to possess better solubility in water with improved reaction rate of S-Au linkage formation. Assuming such a performance for **1**, the double strand DNA (e.g., PCR product) will be, easily detected electrochemically omitting the gel electrophoresis step, thus giving a simple and rapid detection (Figure 1B). Here, we synthesized **1** carrying cysteine at both termini and **2** carrying single cysteine moiety (Figure 1A) and compared their performance. Furthermore, this system

was applied for the detection of PCR product of *P. gingivalis* (*P. g.*), [15] which is important in diagnosis of periodontal disease.

2. Experimental

2.1. Materials.

Naphthalene diimide derivatives **1** and **2** were synthesized by the route of Figure S-1 and S-2. Commercial calf thymus DNA (CT-DNA) purchased from Sigma-Aldrich (St. Louis, MO) partially broken to average size of 1 kilo bases was used all throughout [16]. The concentration of CT-DNA was estimated from the molar absorptivity of $12,824 \text{ cm}^{-1}\text{M}^{-1}$ at 260 nm based on nucleic base pairs [16]. Oligonucleotides used in this study were custom synthesized by Genenet Co. (Fukuoka, Japan) and their concentrations were estimated from the molar absorptivity values (ϵ) as shown in Table 1. PCR product was prepared with primers (FP and RP) and DNA of *P. g.* MES buffer composed of 10 mM MES (pH 6.2), 1 mM EDTA, and 0.10 M NaCl was used in CD measurements, UV-Vis absorption titration experiments, kinetic experiment, and electrochemical measurements. FND was the same as that used previously [11]. 3-Ferrocenylpropanoic acid N-hydroxysuccinimide ester was synthesized as described previously [10]. The composition of $2 \times \text{SSC}$ as a hybridization buffer in the electrochemical experiments was 0.03 M sodium citrate and 0.30 M NaCl. Electrolyte used in electrochemical experiments was 0.10 M NaClO_4 and 0.01 M phosphate ($\text{Na}_2\text{HPO}_4/\text{NaH}_2\text{PO}_4$) buffer (pH 7.0) or 0.10 M AcOK-AcOH buffer (pH 5.5) and 0.10 M KCl containing $50 \mu\text{M}$ of FND.

2.2. Preparation of PCR product.

P. gingivalis chromosomal DNA was extracted from *P. gingivalis* ATCC 33277 in GAM according to the procedure of the illustra bacteria genomic Prep Mini Spin Kit (GE Healthcare). One hundred μL of the reaction solution of PCR was prepared from the following

Table 1. Sequence of oligonucleotides used in this experiment.

	Sequence	$\epsilon/\text{cm}^{-1}\text{M}^{-1}$
ODN1	5'-AGGCTAACTAGCTGCTCATGCGGAGCATTTTACACCTTGAAGAC-3'	420700
ODN2	3'-TCCGATTGATCTACGAGTAC-5'	191100
ODN3	5'-GTCTTCAAGGTGTAATAATGCTCCG-3'	231300
ODN4	5'-CAGAAGTTCCACATTTTACGAGGC-3'	231300
ODN5	NH_2 -5' - TTGTGAATGAAGATGGCGTCGAA-3'	235100
ODN6	5'- TTCGACGCCATCTTCATTCACAA -3'	212600
FP	5'-CTCGTTTCGTACACTTGTCCCG-3'	183800
RP	5'-TTTCTGACCCTGCGTTGTGC -3'	171000

mixture: 50 μL of PrimeSTAR® (Takara Bio Inc., Shiga, Japan, Prime STAR HS DNA polymerase 1.25 units 25 μL , 2 \times dNTP Mixture each 0.4 mM, and 2 \times Prime STAR Buffer 2 mM MgCl_2), 2 μL of *P. gingivalis* chromosomal DNA, 0.4 μM RP, and FP was used for PCR by 45-times repeating the following cycle: 94 $^\circ\text{C}$ for 15 sec, 62 $^\circ\text{C}$ for 5 sec, 72 $^\circ\text{C}$ for 10 sec and 72 $^\circ\text{C}$ for 10 min as final elongation. Sample was pre-heated at 94 $^\circ\text{C}$ for 5 min. After PCR, the product was recovered by PCR Purification kit (QIAGEN).

2.3. Apparatus.

Mass spectra (MS) were taken on a Voyager™ Linear-SA (PerSeptiveBiosystems, Foster City, CA) by the time-of-flight mode with α -cyano-4-hydroxycinnamic acid and 3-hydroxy picolinic acid as matrix for naphthalene diimide derivatives and oligonucleotides respectively. Circular dichroism (CD) spectra were recorded on a Jasco J820 spectropolarimeter (Jasco Inc., Tokyo, Japan). Electronic absorption spectra were recorded with a Hitachi 3300 spectrophotometer equipped with an SPR 10 temperature controller. Kinetic experiments were performed with an SF-61DX2 double mixing stopped flow system (Hi-Tech Scientific, Salisbury, UK) equipped with a Lauda RF206 temperature controller. PCR was carried out using Program temp control system PC-320 (Astec Co., Ltd, Fukuoka, Japan). Electrochemical measurements were carried out with an ALS model 650C electrochemical analyzer (CH Instrument, Austin, TX).

2.4. Immobilization of 1 or 2 in absence or presence of probe dsDNA on the gold electrode.

A gold electrode having a 0.02 cm^2 in theoretical area (BAS, West Lafayette, IN) was polished with 6 μm and 1 μm of a diamond slurry and 0.05 μm of an alumina slurry in this order and sonicated in Milli-Q water for 5 min (3 times). This electrode was electrochemically polished according to the procedure reported by Xiao and co-workers [17], and sonicated in Milli-Q water for 5 min. Air blower dried the pretreated electrode. For 1 or 2 immobilized electrode, 1.5 μL of 100 μM 1 or 2 in MES buffer was placed on the gold electrode held upside down and kept in a closed container under high humidity for 60 min at room temperature. 1-probe dsDNA or 2-probe dsDNA immobilized electrode was prepared by the following procedure. First, 100 μM dsDNA probe was prepared by mixing 100 μM ODN2 with 100 μM ODN1 in 2 \times SSC buffer, and annealing by heating at 90 $^\circ\text{C}$ for 10 min, and cooling to 25 $^\circ\text{C}$ at 0.5 $^\circ\text{C}/\text{min}$. A 1.5 μL of 10 μM 1 or 2 in 10 μM probe dsDNA containing MES

buffer was placed on the gold electrode held upside down and kept in a closed container under high humidity for 60 min at room temperature.

2.5. Immobilization of an ssFcODN or dsFcODN on the gold electrode by 1 or 2.

A 10 μM dsFcODN was prepared by ssFcODN and ODN6. The 10 μM ssFcODN and 10 μM ODN6 in 2 \times SSC were annealed by heating at 90 $^\circ\text{C}$ for 10 min, cooled to 25 $^\circ\text{C}$ at 0.5 $^\circ\text{C}/\text{min}$. A five μL of 2.0 μM ssFcODN or dsFcODN containing 4.0 μM 1 or 2 in MES buffer was placed on the pretreated gold electrode held upside down and kept in a closed container under high humidity for 30 min at room temperature. After the electrode was washed with MES buffer, 100 μL of 1 mM 6-mercaptohexanol (6-MCH) in MES buffer was soaked on the electrode for 10 min at 37 $^\circ\text{C}$. The resulting electrode was washed with MES buffer.

2.6. FND based hybridization assay for the 1-probe dsDNA immobilized electrode with ODN3 or ODN4.

A 1.5 μL of 5.0 μM probe dsDNA, 6.0 μM 1 in MES buffer was placed on the pretreated gold electrode held upside down and kept in a closed container under high humidity for 60 min at room temperature. After the electrode was washed with MES buffer, 100 μL of 1 mM 6-MCH in MES buffer was soaked on the electrode for 30 min at 37 $^\circ\text{C}$. The resulting electrode was washed with MES buffer, and SWV measurement for i_0 was carried out with 50 μM FND in 0.1 M AcOK-AcOH (pH 5.5), 0.1 M KCl. After the electrode was washed with 2 \times SSC, 1.5 μL of 0-10 μM ODN3 or ODN4 in 2 \times SSC was dipped on the 1-probe dsDNA immobilized electrode at 37 $^\circ\text{C}$ for 2h. The SWV measurement for i was carried out with same condition. The current change was evaluated by Δi defined as $(i-i_0)/i_0$.

2.7. Immobilization of PCR products on the gold electrode by 1.

A gold electrode having a 0.01 cm^2 in theoretical area (Tanaka Kikinzoku, Tokyo, Japan) was subjected to O_2 plasma treatment (Cute-MP, Femto Science, Gyeonggi, South Korea) at 0.5 Torr for 30 s. Two μL of 1.0 μM 1 containing various amount of purified PCR products in MES buffer was placed on the gold electrode held upside down and kept in a closed container under high humidity for 30 min at room temperature. After the electrode was washed with MES buffer, 100 μL of 1 mM 6-MCH in MES buffer was soaked on the electrode for 10 min at

37 °C. The resulting electrode was washed with MES buffer.

2.8. Electrochemical measurements.

Cyclic Voltammetry (CV) and Osteryoung square wave voltammetry (SWV) were performed with an ALS 650C electrochemical analyzer. These experiments were carried out with a three-electrode configuration consisting of an Ag/AgCl reference electrode, a Pt counter electrode, and a DNA-immobilized electrode as the working electrode. The following parameters were employed in CV with FcODN immobilized electrode in 0.10 M NaClO₄ and 0.01 M phosphate buffer (pH 7.0): scan rate = 500 mV/s, scan range = -0.1- +0.4 V, segments = 2. The following parameters were employed in SWV with probe dsDNA immobilized electrode in 0.10 M AcOK-AcOH buffer (pH 5.5) and 0.10 M KCl containing 50 μM of FND: applied potential = 10 mV, amplitude = 50 mV, frequency = 10 Hz, sensitivity = 1 x 10⁻⁵ A/V.

3. Results and discussion

3.1. Binding behavior of **1** and **2** with double stranded DNA.

The concentrations of **1** and **2** carrying two and one cysteines, respectively, were estimated by molar absorptivity at 384 nm as $\epsilon=28800 \text{ M}^{-1}\text{cm}^{-1}$. Figure S-3 summarizes the results of the binding analysis for **1** and **2**. Circular dichroic spectra of 80 μM CT-DNA in MES buffer showed negative and positive bands at 246 nm and 274 nm, respectively, which assigned as B-type conformation and they shifted at 239 nm and 278 nm upon addition of 20 μM **2** suggesting its structural change. Furthermore, small negative band was observed around 340 – 400 nm based on naphthalene diimide absorption. Absorption spectra of 10 μM **2** in MES buffer showed small red and large hypochromic shift of 54% upon addition of 0 – 392 μM CT-DNA. On the other hand, absorption spectra of 7.0 μM **1** in MES buffer showed red and hypochromic shifts of 48% based on naphthalene diimide skeleton upon addition of 0 – 315 μM CT-DNA. These behaviors of **1** and **2** are in agreement with naphthalene diimide derivatives which are known as threading intercalators. Further confirmation of the threading intercalation of **1** and **2** was obtained by Topoisomerase I assay or unwinding assay using 25 ng μL⁻¹ (38 μM-bp) of pBR322 plasmid DNA where structural changes of supercoiled plasmid DNA from covalently closed circular (ccc) form to open circular (oc) form were assigned by the band shift in gel electrophoresis (Details are described in SI 1-2) [18]. All

of the experimental results showed threading type intercalation of **1** and **2** with double strand DNA. Binding affinities of both NDI derivatives for calf thymus DNA was estimated by absorption spectra change upon addition of NDI derivatives using McGhee & von Hippel-type Scatchard equation [19] as shown in Table 2. Binding constants of **1** and **2** were $1.2 \times 10^6 \text{ M}^{-1}$ and $7.0 \times 10^5 \text{ M}^{-1}$ with binding site sizes, $n=2.4$ and 2.7 , respectively. Ligand **1** shows two-times higher affinity than that of **2**. As a next step, kinetic analysis of NDI derivatives for calf thymus DNA was carried out to obtain kinetic parameter as summarized in Table 2. Association rate constant of **2** was two-times larger than that of **1** and dissociation rate constant of **2** from CT-DNA was 6-times larger than that of **1**. This came from a fact that **2** has N,N'-dimethyl-1,3-propane diamine and N,N-bis(3-aminopropyl)piperazine linker, whereas **1** has two N,N-bis(3-aminopropyl)piperazine linkers at both terminal. On the other hand, **1** has more bulky substituent than **2** and showed slower association and dissociation with double stranded DNA. Finally, **1** formed more stable

Table 2. Binding parameter of **1**, **2** and **4** with calf thymus DNA

Ligand	K / M ⁻¹	n	k _a / M ⁻¹ s ⁻¹	k _d /s ⁻¹
1	1.2×10^6	2.4	2.8×10^5	0.12
2	7.0×10^5	2.7	6.5×10^5	0.76
4	3.8×10^5	2.1	6.0×10^5	1.09

complex with double stranded DNA than that for **2**.

3.2. Immobilization behavior of **1** or **2** on the gold electrode with or without double strand DNA.

Cyclic voltammetric (CV) measurements were carried out to analyze adsorption behavior of **1** or **2** on the gold surface. Pretreated gold electrode ($\phi = 1.6 \text{ mm}$) was incubated with 1.5 μL of 100 μM **1**, **2**, or amino termini derivative **5** in MES buffer for 60 min and CV of these electrodes were carried out with potential range of -1.3 - 0 V (vs. Ag/AgCl) in 0.01 M phosphate buffer containing 0.10 M NaClO₄. The electrode treated with **5** was observed to have no peak based on the reductive elimination of Au-S linkage, whereas the reduction peaks at -0.96 and -0.95 V were observed for **1** and **2**, respectively (Figure S-4A & B). Furthermore, pretreated gold electrode was incubated with 1.5 μL of 10 μM **1**, or **2** and 10 μM probe dsDNA in MES buffer for 60 min, and CV of these electrodes were carried out. The reduction peaks at -0.94 and -0.93 V were observed for **1**-probe dsDNA and **2**-probe ds DNA, respectively (Figure

S-4C & D). These results suggested that **1** and **2** could be immobilized on the electrode in the presence of DNA. Ulstrup et al. showed the negative shift of the reductive elimination peak potential depending on the packing density of alkyl chains in SAMs [20] and **1** carrying two cysteines termini is expected to be immobilized with higher density than **2** as suggested by the order of redox potential of $\mathbf{1} < \mathbf{2} < \mathbf{1}$ -probe dsDNA < $\mathbf{2}$ -probe dsDNA.

Adsorption behavior of **1** was measured by QCM technique. Frequency change of QCM chip covered with gold (0.049 cm²) was measured in 8 mL of MES buffer and showed immobilization density of 700 pmol cm⁻² of **1**. This result shows that **1** is immobilized on the gold surface more effectively than dithiolane derivative **3** previously reported [10] with immobilization density of 59 pmol cm⁻².

As a next step, DNA immobilization using **1** and **2** was tested by ferrocene-modified oligonucleotides (ssFcODN and dsFcODN). The gold electrode was incubated with MES buffer before being dipped in the 5.0 μ L mixture of 1 μ M 22-meric dsFcODN or ssFcODN and 2 μ M **1** or **2** and subsequently masked with 1 mM 6-MCH, which was used to suppress the electric double layer capacity. Figure 2A-D shows the cyclic voltammograms for ssFcODN and dsFcODN immobilized with **1** and **2** in 0.01 M phosphate buffer containing 0.10 M NaClO₄, over the range of -1.0 – 0.4 V with 0.5 V/s. In the case of double strand DNA immobilization, the electrode treated with dsFcODN-**2** or dsFcODN-**1** showed the ferrocene oxidation and reduction potentials of $E_{pa} = 0.20$ V and $E_{pc} = 0.20$ V with $\Delta E_p (E_{pc} - E_{pa}) = 0$ V, which is one of the evidence of DNA immobilization on the electrode (solid line in Figure 2A & C). On the other hand, the electrode treated with ssFcODN-**1**, ssFcODN-**2** showed the oxidation and reduction potentials of $E_{pa} = 0.25$ V and $E_{pc} = 0.22$ V with $\Delta E_p = 0.03$ V (solid line in Figure 2B & D), which is smaller than that of $\Delta E_p = 0.057$ V for a theoretical value of diffusion process. This result suggested that the complex of dsDNA and ssDNA with **1** or **2** were immobilized on the electrode and in the case of **2**, ssDNA was slightly flexible allowing to move ferrocene moiety on the electrodes to some extent.

To evaluate the stability of DNA immobilized on the electrode by **1** and **2**, CV was measured after treatment with NaOH. The electrode was soaking in 0.5 M NaOH for 5 min and subsequently washing in MES buffer. Current response based on ferrocene was diminished after NaOH treatment. Immobilization density was calculated by the equation of $\Gamma = nFAQ$ where n represents number of electrons per molecule

for reduction ($n = 1$), F Faraday constant, A electrode

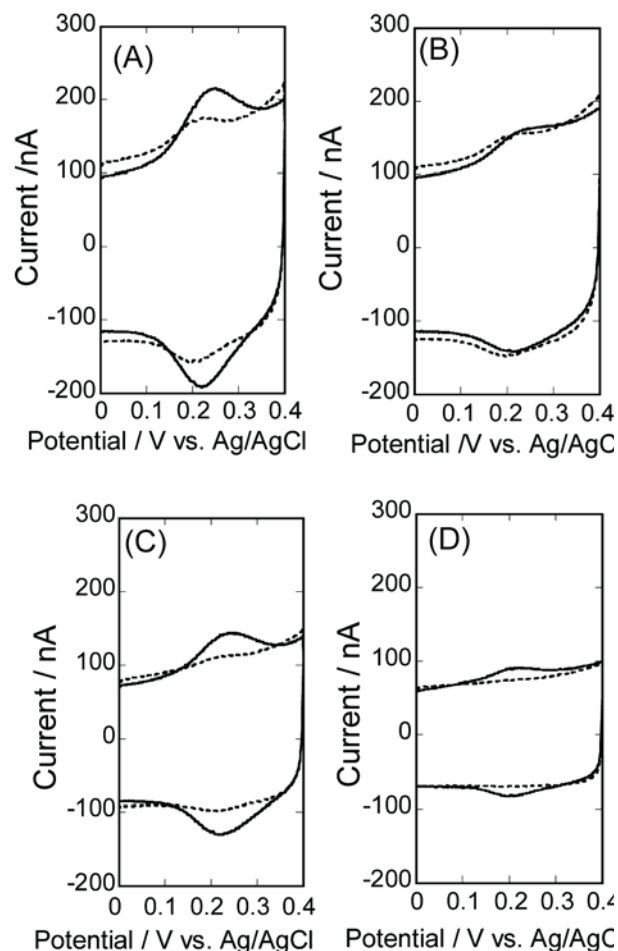


Figure 2. Cyclic voltammograms of the gold electrode treated with **1** in the presence of dsFcODN (A) or ssFcODN (B) or treated with **2** in the presence of dsFcODN (C) or ssFcODN (D) before (solid line) or after (dashed line) immersing in 0.5 M NaOH for 1 min. CV measurements were carried out in 0.1 M NaClO₄, 0.01 M phosphate buffer (pH 7.0) at 25 °C.

area ($A = 0.02$), Q charge [21]. The immobilized amount of DNA after NaOH treatment remained 11, 0, 29, and 42 % in the case of ssFcODN-**2**, dsFcODN-**2**, ssFcODN-**1**, and dsFcODN-**1**, respectively (dashed line in Figure 2A-D). Thus, **1** can immobilize DNA more effectively than **2** and double strand DNA can remain more effectively than single stranded DNA. Immobilization density in the case of dsFcODN-**1** was changed from 5.95×10^{11} molecules cm⁻² to 2.54×10^{11} molecules cm⁻² after NaOH treatment. However, this immobilization density is suitable to carry out hybridization. Finally, **1** can bind to double strand DNA with threading intercalation and the complex can be immobilized on the gold electrode through Au-S

linkage, where DNA can immobilize topologically as shown in Figure 1.

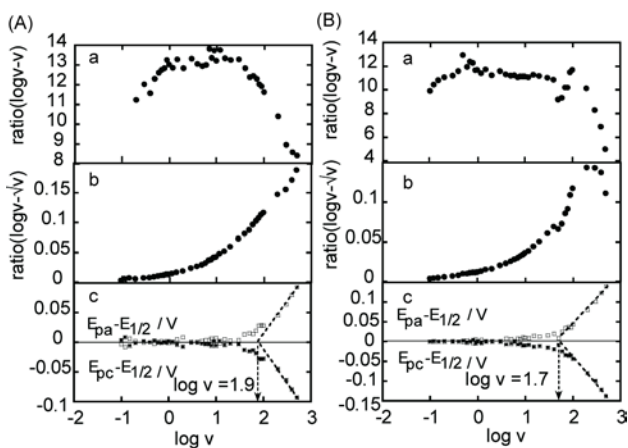


Figure 3. Scan rate ν dependence of the anodic peak current i_{pa} (a, b) and of the anodic and cathodic peak potentials E_{pa} and E_{pc} (c) for cyclic voltammogram recorded at a dsFcODN treated with **1** (A) or **2** (B) immobilized electrode. (a) Anodic peak-current function i_{pa}/ν versus $\log \nu$.

Laviron's plots for the double stranded DNA immobilized by **1** or **2** were carried out to evaluate the mobility of double strand DNA on the electrode [22, 23]. Cyclic voltammograms of the electrode of dsFcODN-**1** or dsFcODN-**2** was measured with a scan rate of 0.01 – 500 V/s. The $i_{pa}/(N_0\nu)/nA$ s/V mol⁻¹ against $\log \nu$ was plotted from the obtained CV data (Figure 3A & B). Nernstian response was kept until $\log \nu = 2.0$ ($\nu = 100$ V/sec) and 1.5 ($\nu = 30$ V/sec) for the dsFcODN electrode immobilized by **2** and **1**, respectively (Fig. 3 panel c). Anne *et al.* reported that the ferrocenyl 20-meric oligonucleotide immobilized electrode showed the Nernstian response until $\log \nu = 4$ and shifted to $\log \nu = 2$ after hybridization [24]. This result suggested that the electrode in the case of dsFcODN-**2** has a flexibility same as the thiolated dsDNA, whereas the electrode in the case of dsFcODN-**1** has a flexibility lower than thiolated dsDNA. Furthermore, there is a peak at $\log \nu = 2.5$ for the electrode for the Fc-dsDNA-**2** in the plot of $i_{pa}/(N_0\nu)/nA$ (s/V)^{0.5} mol⁻¹ against $\log \nu$, whereas no peak was observed in the case of Fc-dsDNA-**1** (panels b in Figure 4). In the case of Anne, the peak at $\log \nu = 2.2$ was observed for double strand DNA, whereas no peak was observed for single strand DNA. It is known that the peak at lower $\log \nu$ showed more rigid structure of DNA on the electrode. In this case, the double strand DNA on the electrode showed similar rigidity. Thus dsFcODN was rigidly or loosely immobilized on the electrode for **1** or **2**, respectively (Figure S-5). Laviron plots was also plotted as $\log \nu$ vs.

$\Delta E_{pa} = E_{pa} - E_{1/2}$ or $\Delta E_{pc} = E_{pc} - E_{1/2}$ [22-24]. Symmetric change of E_{pa} and E_{pc} shows the $\alpha = 0.5$. The ν_c values in the case of **2** and **1** were 50.1 and 79.4 from $\log \nu = 1.7$ and 1.9, respectively. Use of these values enabled calculation of the electron transfer rate of 974 s⁻¹ and 1226 s⁻¹ from the equation of ($k_0 = \alpha n F \nu_c / RT$). It was reported that the thiolated single stranded 15-meric DNA shows 270 s⁻¹ for the electron transfer rate and 40 s⁻¹ [23]. When comparing with this data, dsFcODN immobilized by **1** and **2** shows higher electron transfer rate.

These results show that dsFcODN is immobilized in a restricted form lying on the electrode. To make sure whether double strand DNA was immobilized by **1** or **2**, a probe DNA carrying 24-meric single strand DNA and 20-mer double strand DNA regions was immobilized on the electrode by **1**. The solution of 1.5 μ L of 5.0 μ M the DNA probe with 6.0 μ M **1** in MES buffer was applied on the electrode and incubated at 25 °C for 1 h. After dipping in the solution containing 1 mM 6-MCH in MES buffer the electrode was incubated at 25 °C for 30 min. The obtained electrode was treated with various concentrations of target DNA for 2 h at room temperature and SWV was measured with the electrolyte containing 50 μ M FND in 0.10 M AcOK-AcOH buffer (pH 5.6) containing 0.10 M KCl. As shown in Figure 4A, the current was increased quantitatively in the electrode immobilized the probe-

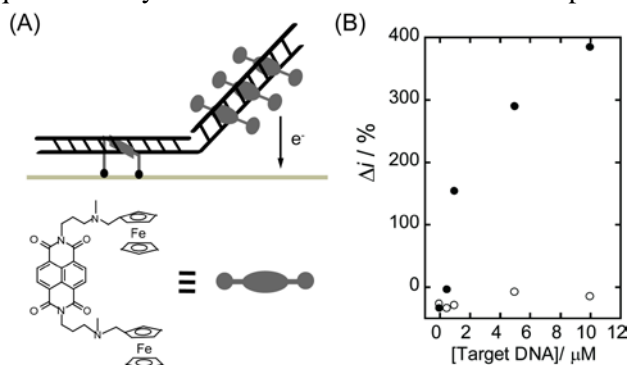


Figure 4. Immobilization of partially double stranded DNA (ODN1 and ODN2) on the electrode by **1** and subsequently hybridization with complementary single stranded DNA (target DNA, ODN3). (A) Expected image of this experiment and (B) the Δi value dependence of the concentration of target DNA (ODN3) (●) or non-complementary single stranded DNA (ODN4) (○).

dsDNA after hybridization of target DNA, whereas no current increase was observed with non-complementary DNA (Figure 4B). This result showed that **1** did not bind to single strand DNA and the single strand DNA part of the immobilized DNA could contribute with effective hybridization.

3.3. Ability of **1** to act as DNA staple.

Cyclic voltammogram of the electrode immobilized with dsFcODN by **1** was measured under different concentration ratios of **1** over dsFcODN. Immobilization time of **1**-dsFcODN at 25 °C was 60 min. As shown in Figure 5A, immobilized amount of dsFcODN increased up to ratio of 2 (**1** over 20 μM dsFcODN) and decreased when ratio value was four or higher. Since **1** was easy to adsorb on the gold surface, increased **1** concentration caused **1** to adsorb on the electrode directly resulting in inhibition of dsFcODN sorption. The effect observed here is similar to that for dithiolane derivative [8]. Immobilization density dependence on dsFcODN concentration was measured under the concentration of 2.0, 3.2 and 4.0 μM **1** (Figure 5C). Linearly dependence of current based on ferrocene was observed in the range of 0.5 – 2.0 μM dsFcODN and reached plateau at high dsFcODN concentration. This result showed that double strand DNA is quantified using constant concentration of **1**. Time dependence of the immobilization efficiency of dsFcODN was measured under 4.0 μM **1** and 2.0 μM dsFcODN as shown in Figure 5B. The dsFcODN was immobilized with density of 5.0×10^{11} molecules cm^{-2} for 10 min and 9.0×10^{11} molecules cm^{-2} for 60 min immobilization period. This time dependence of the immobilized amount was similar as in the case of thiolated DNA previously described [8].

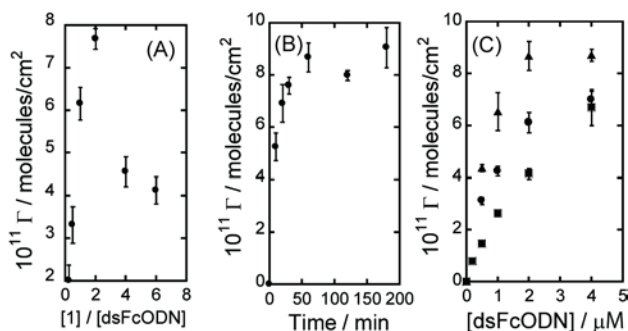


Figure 5. (A) Immobilization density of dsFcODN (Γ) under the varied ratio of **1** to dsFcODN for 1 h at 25 °C, (B) time dependence of the immobilization efficiency, and (C) the dsFcODN concentration effect on the immobilization efficiency in the presence of 2 (\blacksquare), 3.2 (\bullet) and 4 μM (\blacktriangle) of **1**.

3.4. Detection of PCR product using **1**.

It is clear that **1** bound to double stranded DNA and the obtained complex was immobilized on the gold electrode. This technique can be applied to detect PCR product with double strand DNA in the reaction solution. Detection of purified PCR product with in concentration range of 1.0

$\text{pg } \mu\text{L}^{-1}$ – 10 $\text{ng } \mu\text{L}^{-1}$ (1.5 nM - 15 μM) was carried out using **1** as shown in Figure 6. PCR products were mixed with 1.0, 0.5 and 0.2 μM **1**. The obtained solution was applied on the gold electrode and kept for 30 min at 37 °C and subsequently electrode was dipped in 1 mM 6-

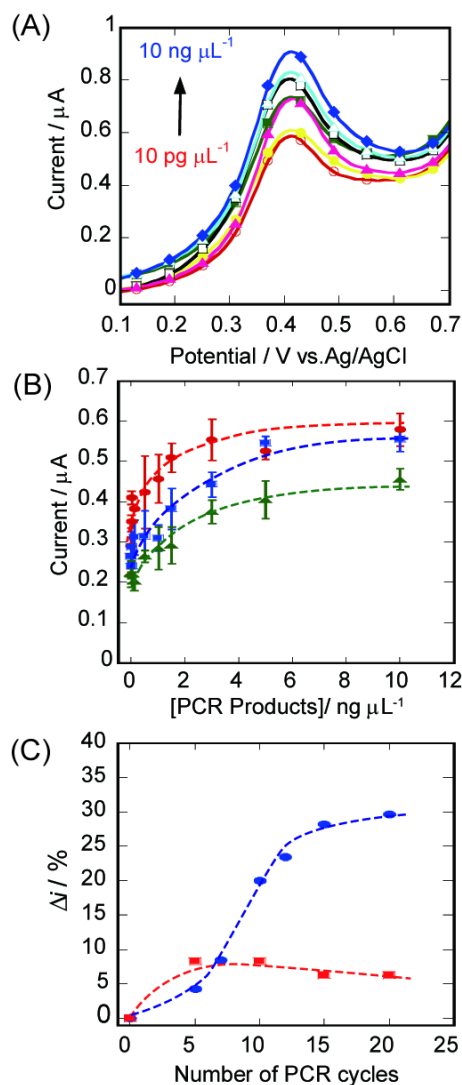


Figure 6. Detection of 321-meric PCR products using **1** and FND as an electrochemical indicator. (A) SWV measurement of the electrode treated with the varied amount of the purified PCR product in the presence of 1.0 μM **1** under the electrolyte consisting with 0.1 M AcOH-AcOH (pH 5.4), 0.1 M KCl, and 50 μM FND. PCR products concentration as follows: 10 $\text{pg } \mu\text{L}^{-1}$ (\circ), 0.1 $\text{ng } \mu\text{L}^{-1}$ (\bullet), 0.5 $\text{ng } \mu\text{L}^{-1}$ (\blacksquare), 1.0 $\text{ng } \mu\text{L}^{-1}$ (\square), 2.0 $\text{ng } \mu\text{L}^{-1}$ (\blacktriangle), 5.0 $\text{ng } \mu\text{L}^{-1}$ (Δ), 10 $\text{ng } \mu\text{L}^{-1}$ (\diamond). (B) Peak current dependence on the concentration of the purified PCR product with 1.0 (\bullet), 0.5 (\blacksquare), 0.2 (\blacktriangle) μM of **1**. (C) Peak current increasing ratio against PCR cycle number in the presence (\bullet) and absence of template DNA (\blacksquare). Peak current was obtained in SWV measurement in the presence of 0.1 μM **1** and the unpurified PCR products under same electrolyte consisting with 0.1 M AcOH-AcOH (pH 5.4), 0.1 M KCl, and 20 μM FND.

MCH at 37 °C for 20 min. SWV of this electrode was measured in 0.1 M AcOK-AcOH and 0.1 M KCl containing 20 μM FND. Since FND bind to double strand DNA on the electrode through threading intercalation, FND can be used to quantify the amount of double strand DNA on the electrode [9-11, 13]. Current peaks based on FND were increased with increase in the concentration of PCR product in the presence of varied amount of **1** (Figure 6A). Slope of current increase of FND per PCR concentration was in the following order: 0.2 μM > 0.5 μM > 1.0 μM of **1**. It is expected that the bound amount of FND per PCR product was increased under small amount of **1** per PCR product (Figure 6B). Since binding amount of **1** per PCR product was 5-times higher in the case of 1.0 μM **1** comparing with 0.2 μM **1**, the slope of the current increase was diminished because of the decreasing number of binding site for FND. Detection limits of PCR product were 0.01, 0.01, and 0.5 $\text{ng } \mu\text{L}^{-1}$ using 1.0, 0.5 and 0.2 μM of **1**, respectively. Detection of PCR product by dye staining after native gel electrophoresis was carried out and the detection limit was 2.0 ng. Although the electrochemical method described here used 2.0 μL of PCR sample, detection limit of gel electrophoresis was 1.0 $\text{ng } \mu\text{L}^{-1}$. Therefore, this method in terms of sensitivity is 100-times higher compared to gel electrophoresis.

PCR products were prepared with various cycle number of PCR and were subsequently placed on the gold electrode with 1.0 μM NDI-C without PCR purification. SWV of this electrode was measured in 0.1 M AcOK-AcOH and 0.1 M KCl containing 20 μM FND. Current peak was increased obviously over 10 PCR cycle in the case of template DNA presence whereas no identical increase was observed in the absence of template DNA as shown in Fig. 6C. Concentration of PCR product under 10 cycle can be estimated as 0.015 $\text{ng } \mu\text{L}^{-1}$ after purification of PCR product, which was in agreement with the detection limit of Figure 6B.

4. Conclusions

1 and **2** were successfully synthesized as naphthalene diimide derivatives carrying two terminal cysteine moieties at both substituents. They bound to double strand DNA as threading intercalator with binding constant of 10^5 M^{-1} order, but **1** possessed higher binding affinity than **2**. This is in agreement with the fact that bulky substituents of naphthalene diimide have higher affinity with double strand DNA with small association and dissociation rate constants [8, 9, 11, 13]. Since our previous works showed that piperazine-type linker chain behaves as a more bulky substituent than dimethylamine one [10, 12], the obtained results are consistent.

Immobilization of single strand DNA on the gold electrode was tested with ssFcODN and **1** or **2** and adsorption of single strand DNA was observed in both cases. Since gold electrode surface is known to be susceptible to non-specific adsorption of ssDNA [25], the excess of ssFcODN was removed by NaOH washing (desorption of non-specifically adsorbed DNA). In the case of double strand DNA, 50% of dsFcODN remained on the electrode after NaOH washing. Conversely, 100 % of the complex of dsFcODN with **2** was removed from the gold electrode with NaOH washing. It is not clear now whether both of two terminal cysteine of **1** bound to dsFcODN did not adsorb on the electrode. Maybe the Au-S linkage was partially cleaved under such strong alkaline conditions. Molecular modeling of **1** estimated the length of its linker chains of 14 Å, which is enough to access the gold surface under complex formation with double strand DNA and it is suggested that the complex of dsFcODN with **1** was more tightly fixed on the electrode than the complex with **2** from the result of Laviron's plot. Immobilization reaction of **1** or **2** on the electrode in the absence or presence of double stranded DNA was faster than that of **3**. This is reasonable from fact that SAM formation rate of alkane thiol is faster than that of disulfide derivative [13].

At the present state, PCR product was detected within 50 min using **1**, which is comparable with conventional gel electrophoresis having 30 min migration and 30 min staining steps. Since double strand DNA was immobilized at about 50 % of the maximum adsorption amount within 10 min using **1** as shown in Figure 5B, the entire procedure time could be shorten to 30 min (10 min of immobilization time and 20 min masking time with 6-MCH). RT-PCR takes longer time than conventional PCR because of the necessity of real time fluorescence measurement. On the other hand, the system described here achieved high sensitivity of 0.01 $\text{ng } \mu\text{L}^{-1}$ and PCR product can be detected under minimal number of PCR cycles (for example 10 PCR cycles) and therefore this system using **1** is expected to accelerate the PCR product detection.

5. Supporting Information

The content of Supporting Information includes the following: experimental procedures (Synthesis of **1**, **2** and ferrocenyloligonucleotide (ssFcODN), Topoisomerase I assay, circular dichroism (CD) spectral measurements, evaluation of the binding ability of **1** with double stranded DNA, and kinetics of binding of **1** with CT-DNA by the stopped-flow technique), and analytical data (Figure S-1-3, S-1-4 and S-1-5).

6. Acknowledgements

This work was supported in part by Grants-in-aid for Scientific Research from the Ministry of Education, Culture, Sports, Science and Technology (MEXT), Japan.

7. References

- [1] J. R. Lakowicz, *Principle of Fluorescence Spectroscopy*, 3rd ed., Springer, Berlin, **2006**.
- [2] P. M. Holland, R. D. Abramson, R. Watson, D. H. Gelfand, *Proc. Natl. Acad. Sci. USA* **1991**, *88*, 7276.
- [3] F. Vitzthum, G. Geiger, H. Bisswanger, H. Brunner, J. Bernhagen, *Anal. Biochem.* **1999**, *276*, 59.
- [4] C. Batchelor-McAuley, G. G. Wildgoose, R. G. Compton, *Biosens. Bioelectron.* **2009**, *24*, 3183.
- [5] E. Paleček, M. Bartošík, *Chem. Rev.* **2010**, *112*, 3427.
- [6] N. Higashi, M. Takahashi, M. Niwa, *Langmuir* **1999**, *15*, 111.
- [7] B. J. Taft, M. A. Lapierre-Devilin, S. O. Kelly, *Chem. Commun.* **2006**, 962.
- [8] S. Sato, A. Hirano, S. Takenaka, *Anal. Chim. Acta* **2010**, *665*, 91.
- [9] S. Takenaka, K. Yamashita, M. Takagi, Y. Uto, H. Kondo, *Anal. Chem.* **2000**, *72*, 1334.
- [10] S. Sato, S. Takenaka, *J. Organomet. Chem.* **2008**, *693*, 1177.
- [11] S. Sato, T. Nojima, M. Waki, S. Takenaka, *Molecules* **2005**, *10*, 693.
- [12] S. Sato, S. Fujii, K. Yamashita, M. Takagi, H. Kondo, S. Takenaka, *J. Organomet. Chem.* **2001**, *637-639*, 476.
- [13] S. Sato, M. Tsueda, Y. Kanazaki, S. Takenaka, *Anal. Chim. Acta* **2012**, *715*, 42.
- [14] H. A. Biebuyck, C. D. Bain, G. M. Whitesides, *Langmuir* **1995**, *10*, 1825.
- [15] A. Ashimoto, C. Chen, I. Bakker, J. Slots, *Oral. Microbiol. Immun.* **1996**, *11*, 266.
- [16] M. W. Davidson, B. G. Griggs, D. W. Boykin, W. D. Wilson, *J. Med. Chem.* **1997**, *20*, 1117.
- [17] Y. Xiao, R. Y. Lai, K. W. Plaxco, *Nat. Protocols* **2007**, *2*, 2875.
- [18] Y. Pommier, J. M. Covey, D. Kerrigan, J. Markovits, R. Pham, *Nucleic Acids Res.* **1987**, *15*, 6713.
- [19] J. D. McGhee, P. H. von Hippel, *J. Mol. Biol.* **1974**, *86*, 469.
- [20] H. Wackerbarth, M. Grubb, J. Zhang, A. G. Hansen, J. Ulstrup, *Angew. Chem. Int. Ed.* **2004**, *43*, 198.
- [21] A. J. Bard, L. R. Faulkner, *Electrochemical Methods*, 2nd ed. Wiley, New York, 2001.
- [22] E. J. Laviron, *Electroanal. Chem.* **1979**, *101*, 19.
- [23] R. Ikeda, S. Kobayashi, J. Chiba, M. Inouye, *Chem. Eur. J.* **2009**, *15*, 4822.
- [24] A. Anne, C. Demaille, *J. Am. Chem. Soc.* **2006**, *128*, 542.
- [25] H. Kimira-Suda, D. Y. Petrovykh, M. J. Tarlov, L. J. Whitman, *J. Am. Chem. Soc.* **2003**, *125*, 9014.